Comparative analysis of fixed-bed sorption models using phosphate breakthrough curves in slag filter media

Chang-Gu Lee[a], Jae-Hyun Kim[b], Jin-Kyu Kang[b], Song-Bae Kim[b,c,]*, Seong-Jik Park[d], Sang-Hyup Lee[a,e], Jae-Woo Choi[a]

[a]Center for Water Resource Cycle Research, Korea Institute of Science and Technology, Seoul 136-791, Korea, emails: changgu@kist.re.kr (C.-G. Lee), yisanghyup@kist.re.kr (S.-H. Lee), plead36@kist.re.kr (J.-W. Choi)
[b]Environmental Functional Materials and Biocolloids Laboratory, Seoul National University, Seoul 151-921, Korea, Tel. +82 2 880 4587; emails: kjh85@snu.ac.kr (J.-H. Kim), naengie@snu.ac.kr (J.-K. Kang), songbkim@snu.ac.kr (S.-B. Kim)
[c]Department of Rural Systems Engineering and Research Institute for Agriculture and Life Sciences, Seoul National University, Seoul 151-921, Korea
[d]Department of Bioresources and Rural Systems Engineering, Hankyong National University, Anseong 456-749, Korea, email: parkseongjik@hknu.ac.kr
[e]Graduate School of Convergence Green Technology and Policy, Korea University, Seoul 136-701, Republic of Korea

ABSTRACT

Fixed-bed kinetic sorption (Bohart–Adams, Thomas, Yoon–Nelson, Clark, Wolborska, and modified dose-response) models are commonly used to simulate breakthrough curves (BTCs) from fixed-bed systems. However, more caution should be taken in using these models. Some researchers misused the equation, which is a totally different type from the original model, as a simplified model. Others used the same equation expressed in different forms as an independent model. The aim of this study was to clarify the fixed-bed sorption models via comparative analysis using the phosphate BTCs in slag filter media. For the analysis, the breakthrough data for phosphate (initial phosphate concentration = 1.0 and 2.0 mg/L) sorption in fixed-bed columns (inner diameter = 2.5 cm and column length = 10, 20, and 30 cm) were obtained from the experiments. The original Bohart–Adams model was simplified in the literature to the convergent- and divergent-type models in order to be used for the BTC analysis. However, the divergent-type model, which is equivalent to the Wolborska model, should not be the type of Bohart–Adams model used, because it behaves totally different from the original model. Also, the Thomas and Yoon–Nelson models should not be used simultaneously with the Bohart–Adams model, because they are equivalent to the simplified convergent-type Bohart–Adams model, and the parameters of both of the models (k_T, q_0, k_{YN}, and τ) can easily be calculated from the Bohart–Adams model parameters (k_{BA} and N_0). The Bohart–Adams, Clark, and modified dose-response models could describe the BTCs relatively well with a high determination coefficient and a low chi-square coefficient. From this study, the Bohart–Adams, Clark, and modified dose-response models are recommended for the BTC analysis, because these models can provide useful design parameters (k_{BA}, N_0, Z_0, t_b, and q_0) for the fixed-bed systems.

*Corresponding author.

1. Introduction

The adsorption characteristics of a contaminant to an adsorbent can be examined via batch sorption tests and dynamic fixed-bed experiments. Batch tests are usually conducted in order to determine the effectiveness of a specific adsorbent for removing a target adsorbate and to quantify the maximum adsorption capacity from the sorption isotherm. Batch tests are usually performed as a preliminary screening of the adsorbent before continuous column experiments, because accurate scale-up data for fixed-bed systems cannot be provided from batch tests [1,2]. Fixed-bed experiments are conducted under continuous flow conditions in order to obtain the characteristic parameters for fixed-bed systems. The performance of fixed-bed columns can be described in terms of time vs. effluent concentration (breakthrough curve (BTC)). The breakthrough time and BTC shape are important characteristics for determining the operation of fixed-bed columns [3,4]. The BTCs must be predicted successfully via quantitative models in order to design and optimize the fixed-bed systems [5,6].

Various simple mathematical models have been developed for this purpose (Table 1). Bohart and Adams [7] developed a model based on the assumption that the adsorption rate is proportional to both the residual capacity of the adsorbent and the concentration of the adsorbate. Although the model was originally developed to describe the adsorption of chlorine on charcoal in a fixed-bed column, it has been successfully applied to the quantitative description of other systems [4,8]. Thomas [9,10] developed a model using the Langmuir equilibrium isotherm and second-order reversible reaction kinetics with the assumption of plug flow behavior (zero longitudinal dispersion) in the fixed-bed. Yoon and Nelson [11] developed a relatively simple model based on the assumption that the rate of decrease in the probability of the adsorption of the adsorbate molecule was proportional to the probability of the adsorbate adsorption and the adsorbate breakthrough on the adsorbent. Clark [12] developed a more refined model to simulate BTCs using the mass-transfer concept and the Freundlich equilibrium isotherm. Wolborska [13] proposed a model to describe the concentration distribution of the adsorbate in the fixed-bed in the range of the low-concentration BTCs. Yan et al. [14] presented a modified dose-response model to more adequately describe the breakthrough data than the Bohart–Adams and Thomas models.

Literature showed that these fixed-bed sorption models have been used by many researchers for the simulation of breakthrough data from the various fixed-bed systems [15–19]. However, more caution

Table 1
Nonlinear and linear forms of the fixed-bed sorption models used in analysis

Model	Nonlinear form	Linear form	Eq. no.	Reference
Bohart–Adams	$\frac{C_t}{C_0} = \frac{e^{k_{BA}C_0 t}}{e^{k_{BA}N_0 \frac{Z}{U}} - 1 + e^{k_{BA}C_0 t}}$	$\ln\left(\frac{C_0}{C_t} - 1\right) = \ln\left[\exp\left(k_{BA}N_0\frac{Z}{U}\right) - 1\right] - k_{BA}C_0 t$	(1)	[7]
	$\frac{C_t}{C_0} = \frac{1}{e^{k_{BA}N_0\frac{Z}{U} - k_{BA}C_0 t} + 1}$	$\ln\left(\frac{C_0}{C_t} - 1\right) = k_{BA}N_0\frac{Z}{U} - k_{BA}C_0 t$	(2)	[7]
	$\frac{C_t}{C_0} = e^{k_{BA}C_0 t - k_{BA}N_0\frac{Z}{U}}$	$\ln\frac{C_t}{C_0} = k_{BA}C_0 t - k_{BA}N_0\frac{Z}{U}$	(3)	[24]
		$t = \frac{N_0}{C_0 U}Z - \frac{1}{k_{BA}C_0}\ln\left(\frac{C_0}{C_t} - 1\right)$	(4)	[26]
Thomas	$\frac{C_t}{C_0} = \frac{1}{e^{\frac{k_T q_0 X}{Q} - k_T C_0 t} + 1}$	$\ln\left(\frac{C_0}{C_t} - 1\right) = \frac{k_T q_0 X}{Q} - k_T C_0 t$	(5)	[10]
Yoon–Nelson	$\frac{C_t}{C_0} = \frac{1}{e^{k_{YN}(\tau - t)} + 1}$	$\ln\left(\frac{C_0}{C_t} - 1\right) = k_{YN}\tau - k_{YN}t$	(6)	[11]
Clark	$\frac{C_t}{C_0} = \left(\frac{1}{Ae^{-rt} + 1}\right)^{\frac{1}{n-1}}$	$\ln\left[\left(\frac{C_0}{C_t}\right)^{n-1} - 1\right] = -rt + \ln A$	(7)	[12]
Wolborska	$\frac{C_t}{C_0} = e^{\frac{\beta C_0}{N_0}t - \frac{\beta Z}{U}}$	$\ln\frac{C_t}{C_0} = \frac{\beta C_0}{N_0}t - \frac{\beta Z}{U}$	(8)	[13]
Modified dose-response	$\frac{C_t}{C_0} = 1 - \frac{1}{\left(\frac{C_0 Q t}{q_0 X}\right)^a + 1}$	$\ln\left(\frac{C_t}{C_0 - C_t}\right) = a\ln(t) + a\ln\left(\frac{C_0 Q}{q_0 X}\right)$	(9)	[14]

should be taken in using these models to simulate BTCs obtained from fixed-bed experiments. Some researchers misused the equation, which is a totally different type from the original model, as a simplified model. Others used the same equation expressed in different forms as an independent model to simulate breakthrough data [20]. Therefore, it is necessary to clarify the models used in the fixed-bed systems. Phosphate removal from aqueous solutions is essential for protecting the aquatic environments from eutrophication [21]. Iron/steel slags, by-products of iron/steel manufacturing, have been applied for the removal of phosphate from aqueous solutions [22]. In this study, six models (Bohart–Adams, Thomas, Yoon–Nelson, Clark, Wolborska, and modified dose-response) were compared using the breakthrough data for phosphate sorption in fixed-bed columns containing slag filter media. The simulated BTCs and model parameters obtained from the simulations were presented.

2. Materials and methods

2.1. Slag filter media

Steel slag (Ecomaister Co., Incheon, Korea) was used as filter media in the experiments. Prior to use, the slag was prepared by mechanical sieving through US Standard Sieves No. 30 and No. 20 (grain size: 0.59–0.84 mm) and was washed twice with deionized water in order to remove surface impurities. The wet materials were oven-dried at 105°C overnight. The chemical composition and surface characteristics of the slag were reported in our previous study [22]. Briefly, X-ray fluorescence analysis indicated that the slag was composed of calcium (40.7%) and iron (25.1%) as well as silica, magnesium, aluminum, and manganese. The X-ray diffractometer pattern demonstrated that dicalcium ferrite ($Ca_2Fe_2O_5$), magnetite (Fe_3O_4), and hematite (Fe_2O_3) were the major constituents [22].

2.2. Batch sorption experiments

The stock solution of phosphate (1,000 mg/L) was prepared by dissolving reagent-grade potassium dihydrogen phosphate (KH_2PO_4) into deionized water. In this experiment, the initial phosphate concentration was adjusted to 2 mg/L phosphorous (P) by diluting the stock solution. Batch experiments were conducted in order to examine the phosphate removal by the slag. Batch experiments were performed in a 50 mL polypropylene conical tube. The experiments were carried out with slag concentrations ranging from 0.12 to 1.5 g in 30 mL of the solution. The tubes were shaken at 30°C and 100 rpm using a shaking incubator (Daihan Science, Korea). The slag was separated from the solution using a permanent magnet (≈1.18 Tesla) 18 h post-reaction. The phosphate was analyzed by the ascorbic acid method [23]. The phosphate concentrations were measured at a wavelength of 880 nm using a UV–vis Spectrophotometer (GENESYS 10S, Thermo Fisher Scientific Inc., Madison, WI, USA). The batch experiments were performed in triplicate.

2.3. Fixed-bed sorption experiments

The fixed-bed sorption experiments were performed using a Plexiglas column (inner diameter = 2.5 cm, column length = 10, 20, and 30 cm) packed with slag (particle density = 3.53 g/cm³). The experimental conditions are provided in Table 2. Each column experiment employed a separate column packed with slag by the tap-fill method. Prior to the experiments, the packed column was flushed upward using a connected peristaltic pump (QG400, Fluid Metering Inc., Syosset, NY, USA) for 20 pore volumes of deionized water until steady-state flow conditions were established. Then, the phosphate solution was introduced downward into the packed column at the same flow rate in a step injection mode. Portions of the effluent were collected using an auto collector (Retriever 500, Teledyne, City of Industry, CA, USA) at regular intervals and the phosphate concentration was analyzed. The effluent pH was measured with a pH probe (9107BN, Thermo Scientific, Waltham, MA, USA) and the electrical conductivity (EC) was measured with an EC probe (815PDL, Istek, Korea).

2.4. Data analysis

All of the parameters of the models were estimated using MS Excel 2010 with solver add-in function incorporated into the program. The determination coefficient (R^2), chi-square coefficient (χ^2), and sum of square error (SSE) were used to analyze the data and confirm the fit to the model. The expressions of R^2, χ^2, and SSE are given below:

$$R^2 = \frac{\sum_{i=1}^{m}(y_c - \bar{y}_e)_i^2}{\sum_{i=1}^{m}(y_c - \bar{y}_e)_i^2 + \sum_{i=1}^{m}(y_c - y_e)_i^2} \quad (10)$$

$$\chi^2 = \sum_{i=1}^{m}\left[\frac{(y_e - y_c)^2}{y_c}\right]_i \quad (11)$$

Table 2
Fixed-bed experimental conditions for the phosphate sorption to slag filter media

Experiment	C_0 (mg/L)	U (cm/min)	Q (L/min)	Z (cm)	Bed volume (cm^3)	EBCT (min)	Pore volume (cm^3)	Bulk density (g/cm^3)	Mass of adsorbent (g)	pH$_{effluent}$ (−)	EC$_{effluent}$ (μS/cm)
1	2.0	3.33	0.0163	10	49.09	3	16.36	2.24	110	7.46 ± 0.04	44.41 ± 1.42
2	2.0	3.33	0.0163	20	98.17	6	32.72	2.24	220	7.83 ± 0.12	44.42 ± 2.02
3	2.0	3.33	0.0163	30	147.26	9	49.09	2.24	330	8.00 ± 0.20	59.07 ± 10.56
4	2.0	1.67	0.0082	20	98.17	12	32.72	2.24	220	8.14 ± 0.18	57.35 ± 10.85
5	1.0	3.33	0.0163	20	98.17	6	32.72	2.24	220	9.39 ± 0.16	52.60 ± 3.19

Notes: EBCT: empty-bed contact time; pore volume = bed volume—particle volume; particle volume = mass of adsorbent/particle density of adsorbent; EC: electrical conductivity.

$$SSE = \sum_{i=1}^{m} (y_e - y_c)_i^2 \qquad (12)$$

3. Results and discussion

3.1. Phosphate BTCs

The BTCs obtained from the fixed-bed experiments are shown in Fig. 1. With increasing column length, i.e. the bed height from 10 cm (experiment 1) to 30 cm (experiment 3), the BTCs became less steep and saturation was achieved more slowly. The longer column length leads to more dispersed BTCs, that is, increasing the column length broadens the mass-transfer zone, resulting in a decrease of the BTC slope [24]. Increasing the column length also decreased the concentration of phosphate in the effluent as a result of an increase in the contact time for phosphate adsorption to slag filter media. Note that EBCT increased from 3 to 9 min as the column length was increased from 10 to 30 cm. With increasing column length, the

Fig. 1. BTCs of the phosphate obtained from the fixed-bed experiments.

phosphate adsorption capacity of slag increased from 1.6 mg/g (experiment 1) to 20.0 mg/g (experiment 3).

In addition, with increasing flow rate from 0.0082 L/min (experiment 4) to 0.0163 L/min (experiment 2), steeper BTCs and higher saturation concentration were observed. As the flow rate increases, the contact time between the phosphate and the filter medium decreases. In our experiments, EBCT decreased from 12 min (experiment 4) to 6 min (experiment 2) as the flow rate was increased (column length = 20 cm). As the flow rate increases, the BTC becomes steeper because the driving forces increase, leading to a decrease in the adsorption zone length [24]. Increasing the flow rate decreased the phosphate adsorption capacity from 47.0 mg/g (experiment 4) to 6.5 mg/g (experiment 2). With increasing phosphate concentration from 1.0 mg/L (experiment 5) to 2.0 mg/L (experiment 2), the BTCs became steeper and saturation was achieved more quickly. As the influent concentration increased, the phosphate adsorption capacity decreased from 18.0 mg/g (experiment 5) to 6.5 mg/g (experiment 2).
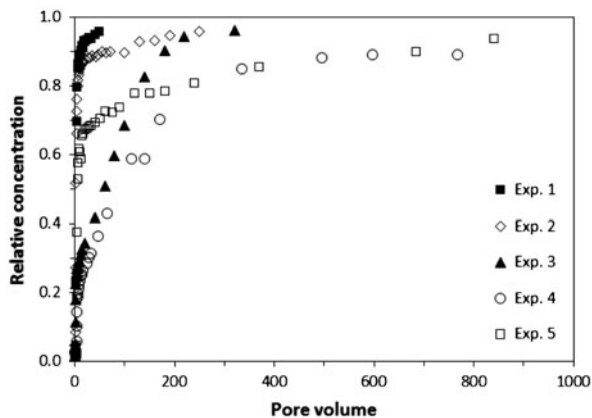
3.2. Clarification of the Bohart–Adams model

The nonlinear and linear forms of the Bohart–Adams model are presented in Table 1. The nonlinear form of Eq. (2) was simplified from Eq. (1) when the second term in the denominator (=1) was entirely negligible except for very small values of both $k_{BA}N_0Z/U$ and $k_{BA}C_0t$. The original (Eq. (1)) and simplified (Eq. (2)) versions were used in order to simulate the BTCs of the phosphate (Fig. 1) obtained from the fixed-bed experiments. Nonlinear regression was performed in order to simulate the BTCs using the nonlinear forms of the Bohart–Adams model.

The experimental BTCs along with the simulated BTCs of Eq. (1) are presented in Fig. 2(a). The model parameters (k_{BA} and N_0) determined from the simulations are presented in Table 3. As shown in the
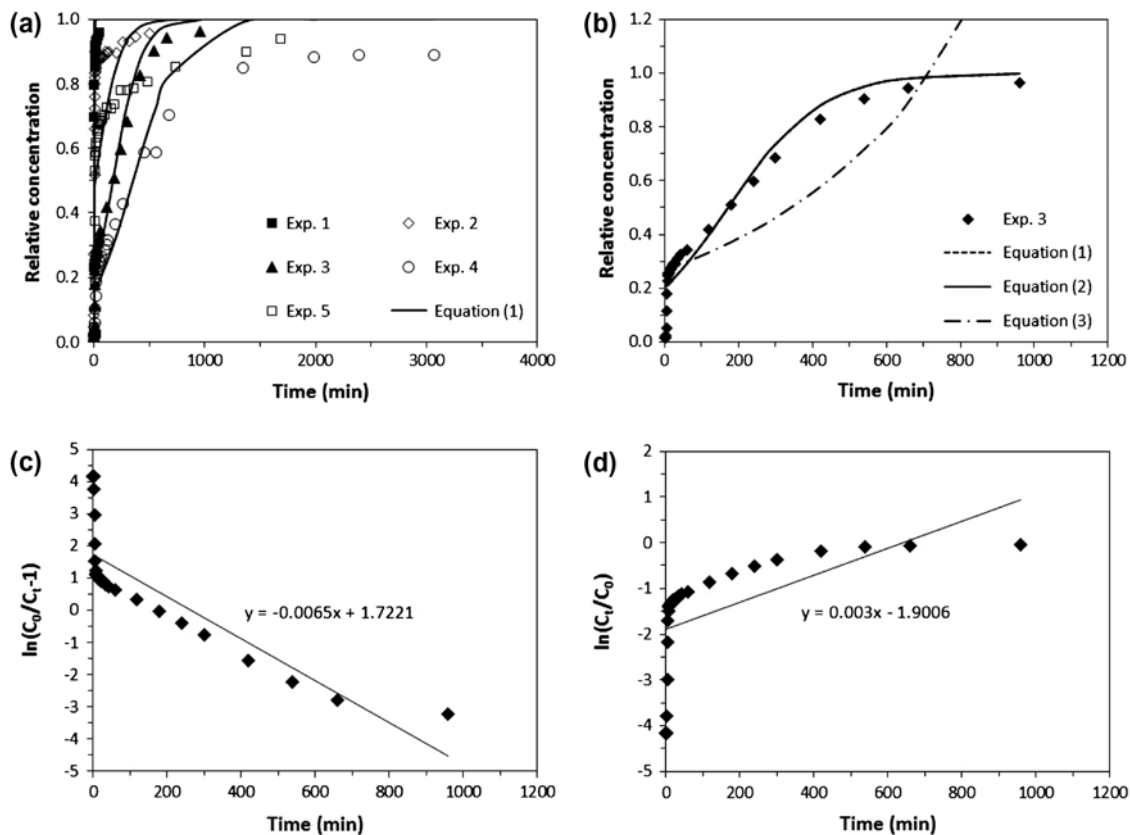
Fig. 2. The Bohart–Adams model analysis: (a) nonlinear regression using Eq. (1); (b) nonlinear regression using Eqs. (1)–(3) for experiment 3; (c) linear regression using Eqs. (1) and (2) for experiment 3; (d) linear regression using Eq. (3) for experiment 3. Note that model fits of Eq. (2) were superimposed on the fits of Eq. (1) in (b) and (c).

example (experiment 3) in Fig. 2(b), the simulated BTC of Eq. (2) was superimposed on the simulated BTC of Eq. (1). In the case of k_{BA}, the same values were obtained from Eqs. (1) and (2). However, different values of N_0 were quantified (Table 3). Linear regression was also conducted using the linear forms of Eqs. (1) and (2) (Fig. 2(c)). The parameter values of k_{BA} and N_0 of the linear regression were quite different from the values of the nonlinear regression. In Eq. (2), negative values of N_0 were quantified by linear regression from experiments 1, 2, and 5 (Table 3). The values of R^2, χ^2, and SSE indicated that the nonlinear regression was far better at simulating the BTCs than the linear regression.

Several researchers have used Eq. (3) (Table 1) as the Bohart–Adams model in order to analyze the breakthrough data [5,15,17,25,26]. Aksu and Gönen [8] applied Eq. (3) in order to describe the initial portion of the breakthrough data of phenol obtained from the continuous packed-bed study. Han et al. [3] also used Eq. (3) to simulate only the initial portion of the BTCs of methylene blue. However, Eq. (3) is totally different

from the original (Eq. (1)) and simplified (Eq. (2)) versions of the Bohart–Adams model. Eq. (3) is a divergent-type model, whereas Eqs. (1) and (2) are convergent-type models. As shown in Fig. 2(b), Eq. (3) was not suitable for the simulation of the entire BTC of the phosphate and behaved differently from Eqs. (1) and (2). Also, the model parameters (k_{BA} and N_0) from Eq. (3) were different from those from Eqs. (1) and (2) (Table 3). Linear regression was also conducted using the linear form of Eq. (3) (Fig. 2(d)).

The nonlinear form of the Bohart–Adams model Eq. (2) was linearized and rearranged by Hutchins [27] into Eq. (4) (Table 1). Eq. (4) can also be written as the following equation:

$$t_b = \frac{N_0}{C_0 U} Z - \frac{1}{k_{BA} C_0} \ln\left(\frac{C_0}{C_b} - 1\right) \qquad (13)$$

Eq. (13) is called the bed depth service time (BDST) model and is widely used to describe the relationship between the breakthrough time (t_b) and the bed depth (Z) for fixed-bed systems. The breakthrough time is

Table 3
The Bohart–Adams model parameters (Eqs. (1)–(3))

Experiment	Nonlinear analysis					Linear analysis				
	k_{BA} (L/min/mg)	N_0 (mg/L)	R^2	χ^2	SSE	k_{BA} (L/min/mg)	N_0 (mg/L)	R^2	χ^2	SSE
Eq. (1)										
1	1.00254	1.764	0.978	0.172	0.162	0.03690	3.872	0.425	1.064	0.730
2	0.38163	1.794	0.971	0.447	0.400	0.00325	19.303	0.257	2.399	1.670
3	0.00398	44.395	0.906	1.003	0.221	0.00325	64.431	0.880	1.719	0.338
4	0.00236	65.099	0.927	0.943	0.238	0.00085	189.244	0.766	2.646	0.624
5	0.00920	13.450	0.525	1.359	0.741	0.00190	56.946	0.365	1.636	0.882
Eq. (2)										
1	1.00254	1.762	0.978	0.172	0.162	0.03690	−5.630	0.425	1.064	0.730
2	0.38163	1.783	0.971	0.447	0.400	0.00325	−40.052	0.257	2.399	1.670
3	0.00398	38.056	0.906	1.003	0.221	0.00325	58.816	0.880	1.719	0.338
4	0.00237	58.976	0.927	0.943	0.238	0.00085	173.778	0.766	2.646	0.624
5	0.00920	1.766	0.525	1.359	0.741	0.00190	−7.764	0.365	1.636	0.882
Eq. (3)										
1	0.00407	24.439	0.233	1.194	0.909	0.01280	19.972	0.181	2.574	1.756
2	0.00040	124.614	0.158	2.511	1.878	0.00105	100.677	0.134	4.324	2.661
3	0.00091	160.342	0.632	1.907	0.888	0.00150	140.644	0.500	4.099	3.601
4	0.00027	411.714	0.591	2.533	0.991	0.00045	369.924	0.484	5.321	2.628
5	0.00033	249.999	0.266	1.657	1.021	0.00070	189.001	0.237	2.770	1.563

the time when the effluent concentration reaches the value of the current legislation limit of a specific contaminant. At $t_b = 0$, Eq. (13) can be rearranged in order to calculate the critical-bed depth (Z_0), which is defined as the minimum bed depth required to obtain a desired effluent quality at time zero, and can be determined using the following equation [27]:

$$Z_0 = \frac{U}{k_{BA} N_0} \ln\left(\frac{C_0}{C_b} - 1\right) \qquad (14)$$

The BDST plot for phosphate adsorption by the slag filter media is presented in Fig. 3. In the BDST plot, N_0 can be quantified from the slope, whereas k_{BA} can be quantified from the intercept. At the given experimental conditions (initial phosphate concentration = 2.0 mg/L, linear velocity = 3.3 cm/min), the values of k_{BA} and N_0 were 0.22980 L/min/mg and 2.521 mg/L, respectively. At $C_b = 0.5$ mg/L, the critical-bed depth for the slag filter media (Z_0) was calculated to be 6.315 cm using Eq. (14), corresponding to the intercept of the X-axis in Fig. 3. Eq. (4) can be further simplified at the time for 50% breakthrough ($t_{50\%}$; $C_t = 0.5C_0$), because the second term on the right side of Eq. (4) becomes zero:
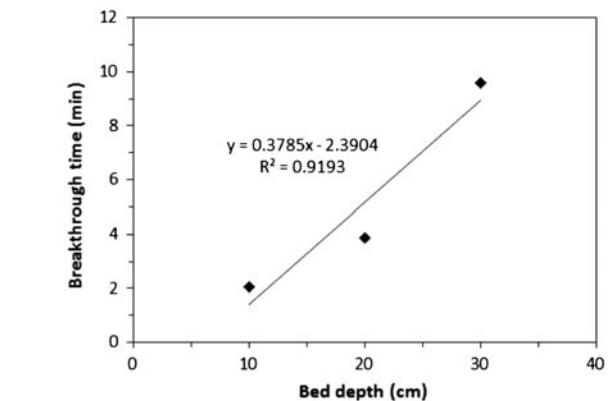

Fig. 3. The BDST plot for the phosphate adsorption to slag filter media.

$$t_{50\%} = \frac{N_0 Z}{C_0 U} \qquad (15)$$

It should be noted that Eq. (15) appears again in Eq. (21) in a later section of this paper.

3.3. Equivalence of the Bohart–Adams model to other models

Eq. (5) developed by Thomas in 1948 [10] is mathematically equivalent to the simplified version of the Bohart–Adams Eq. (2) (Table 1). Chu [20] clearly showed that the model parameters (k_T and q_0) of the Thomas model could be calculated from the Bohart–Adams model parameters (k_{BA} and N_0) with the following relationships:

$$K_{BA}N_0\frac{Z}{U} - k_{BA}C_0t = \frac{k_Tq_0X}{Q} - k_TC_0t \quad (16)$$

$$k_T = k_{BA} \quad (17)$$

$$q_0 = \frac{N_0ZS}{1000X} \quad (18)$$

It should be noted that ZS is the volume of the fixed-bed column and ZS/X is the reciprocal of the bulk density of the adsorbent (ρ_b). Therefore, q_0 is easily calculated when N_0 is divided by $\rho_b \times 10^3$. The values of k_T and q_0 determined from the fitting of the Thomas model to the breakthrough data (Table 4) were comparable with the values calculated from the Bohart–Adams parameters (k_{BA} and N_0).

Eq. (6) was developed by Yoon and Nelson in 1984 [11]. As is the case in the Thomas model, Eq. (6) is also mathematically equivalent to the Bohart–Adams model Eq. (2) (Table 1). The model parameters (k_{YN} and τ) of the Yoon–Nelson model can easily be calculated from the Bohart–Adams model parameters (k_{BA} and N_0) with the following relationships:

$$k_{YN}(\tau - t) = k_{YN}\tau - k_{YN}t = k_{BA}N_0\frac{Z}{U} - k_{BA}C_0t \quad (19)$$

$$k_{YN} = k_{BA}C_0 \quad (20)$$

$$\tau = \frac{N_0Z}{C_0U} = \frac{N_0ZS}{1000C_0Q} \quad (21)$$

It should be noted that Eq. (21) is equal to Eq. (15). The values of k_{YN} and τ from the fitting of the Yoon–Nelson model to the breakthrough data (Table 4) are comparable with the values calculated from the Bohart–Adams parameters (k_{BA} and N_0). In addition, the Yoon–Nelson model parameters (k_{YN} and τ) can easily be calculated from the Thomas model parameters (k_T and q_0), because they are also equivalent to each other as shown in the following equations:

$$k_{YN} = k_TC_0 \quad (22)$$

$$\tau = \frac{q_0X}{C_0Q} \quad (23)$$

It should be noted that R^2, χ^2, and SSE match exactly in Eqs. (2), (5), and (6), but the parameters for each model represent different constants (Table 4).

Eq. (8) is the Wolborska model, which was developed in 1989 [13]. Several researchers used the Wolborska model in order to analyze the breakthrough data [2,6,17,19,28]. It should be noted that Eq. (8) is mathematically equivalent to Eq. (3) with the following relationship:

Table 4
Comparison of the Thomas and Yoon–Nelson model parameters with parameters from the Bohart–Adams model Eq. (2) (Experiment 3)[*]

Bohart–Adams model Eq. (2)				
k_{BA} (L/min/mg)	N_0 (mg/L)	R^2	χ^2	SSE
0.00398	38.056	0.906	1.003	0.221
Thomas model Eq. (5)				
k_T (L/min/mg)	$q_0 \times 10^3$ (mg/g)	R^2	χ^2	SSE
0.00398	17.00	0.906	1.003	0.221
Yoon–Nelson model Eq. (6)				
k_{YN} (1/min)	τ (min)	R^2	χ^2	SSE
0.00796	171.416	0.906	1.003	0.221

[*]The model parameters are from nonlinear regression analysis.
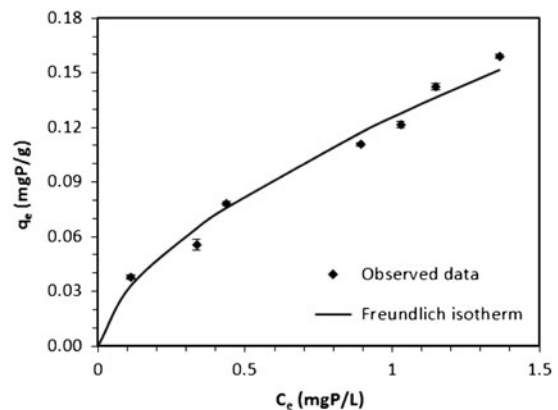

Fig. 4. The Freundlich isotherm model analysis for the phosphate adsorption data from the batch experiment.
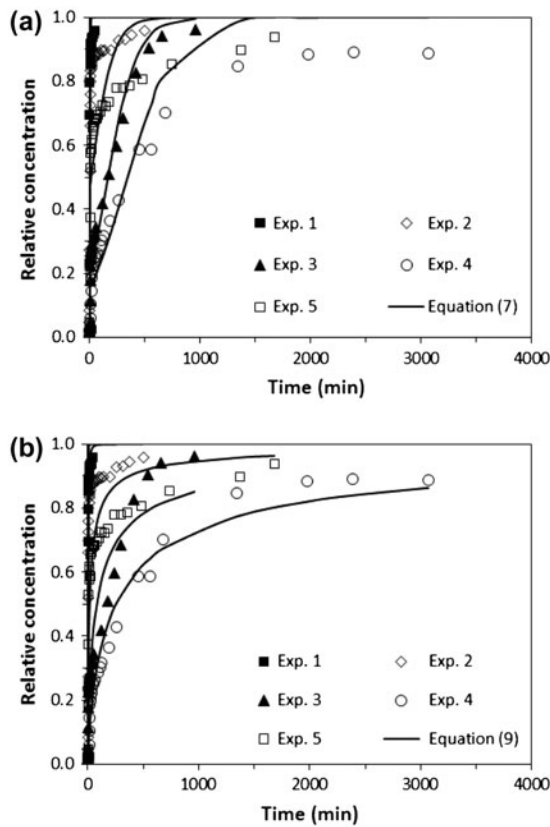
Fig. 5. Nonlinear regression analysis using: (a) Clark model Eq. (7); (b) modified dose-response model Eq. (9).
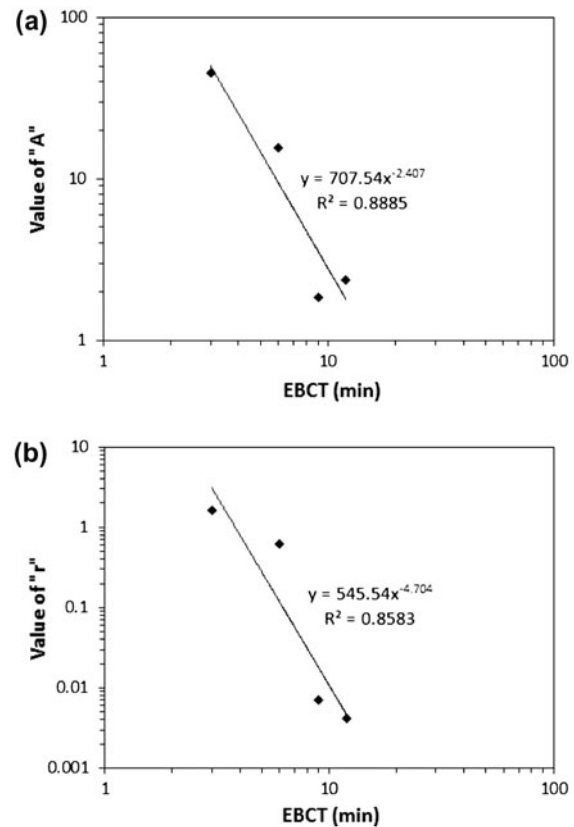

Fig. 6. Plots for the empty-bed contact time (EBCT) vs. the Clark model parameters of (a) A and (b) r.

$$\frac{\beta C_0 t}{N_0} - \frac{\beta Z}{U} = k_{BA} C_0 t - k_{BA} N_0 \frac{Z}{U} \tag{24}$$

$$\beta = k_{BA} N_0 \tag{25}$$

It should also be noted that β is the lumped parameter of the Bohart–Adams model. The nonlinear and linear regressions were performed in order to simulate the

BTCs using the nonlinear and linear forms of the Bohart–Adams model (simulated BTCs were not shown). The value of β from the fitting of the Wolborska model to the breakthrough data are comparable with the value calculated from the parameters (k_{BA} and N_0) of Eq. (3). Also, the fitted values of N_0 (data not shown) were equal to the values in Eq. (3). As is the case in Eq. (3), the Wolborska model, which is the divergent-type model, did not simulate the entire BTC of phosphate very well.

Table 5
The Clark model parameters (Eq. (7))

Experiment	Nonlinear analysis					Linear analysis				
	A (–)	r (1/min)	R^2	χ^2	SSE	A (–)	r (1/min)	R^2	χ^2	SSE
1	44.978	1.6527	0.979	0.160	0.154	0.290	0.0677	0.427	1.070	0.754
2	15.655	0.6176	0.970	0.433	0.382	0.258	0.0061	0.259	2.384	1.694
3	1.832	0.0071	0.908	0.987	0.213	2.338	0.0058	0.890	1.500	0.290
4	2.366	0.0042	0.932	0.910	0.227	2.390	0.0015	0.790	2.226	0.543
5	0.643	0.0094	0.539	1.347	0.731	0.499	0.0017	0.368	1.591	0.874

Table 6
The modified dose-response model parameters (Eq. (9))

| | Nonlinear analysis | | | | | Linear analysis | | | | |
Experiment	a (–)	$q_0 \times 10^3$ (mg/g)	R^2	χ^2	SSE	a (–)	$q_0 \times 10^3$ (mg/g)	R^2	χ^2	SSE
1	3.629	0.799	0.977	0.119	0.107	1.379	0.847	0.853	0.421	0.185
2	2.188	0.813	0.952	0.395	0.255	0.828	0.886	0.800	1.036	0.464
3	0.704	7.998	0.929	0.539	0.158	0.953	6.850	0.910	0.933	0.247
4	0.741	18.938	0.975	0.274	0.058	0.863	17.763	0.972	0.384	0.070
5	0.715	1.282	0.845	0.618	0.248	0.667	2.073	0.807	0.858	0.309

3.4. Analysis with the Clark and modified dose-response models

Before analysis of the BTCs using the Clark model, the Freundlich constant ($1/n$) was determined from the batch sorption data, which were analyzed by the Freundlich isotherm model as follows:

$$q_e = K_F C_e^{1/n} \tag{26}$$

As is shown in Fig. 4, the batch data were described well by the Freundlich model ($R^2 = 0.978$; $\chi^2 = 0.0033$; SSE = 0.00028). The model parameters of K_F and $1/n$ were determined to be 0.126 and 0.607 L/g, respectively. The value of ($n = 1.647$) determined from the analysis was used for the Clark model. The nonlinear and linear regressions were performed in order to simulate the BTCs. The experimental BTCs along with the simulated BTCs of the nonlinear form of the Clark model are presented in Fig. 5(a). The model parameters (A and r) determined from the simulations are presented in Table 5. The parameter values of A and r of the linear regression were quite different from the values of the nonlinear regression. The values of R^2, χ^2, and SSE indicated that the nonlinear regression was far better at simulating the BTCs. In order to calculate the breakthrough time (t_b) from the Clark model, Eq. (7) can be rearranged as follows:

$$t_b = \frac{1}{r} \ln \left[\frac{A}{\left(\frac{C_0^{n-1}}{C_b^{n-1}} - 1 \right)} \right] \tag{27}$$

Based on the values of A and r determined from the nonlinear analysis (experiments 1–4), two plots of EBCT vs. A and EBCT vs. r were obtained (Fig. 6). By choosing a specific EBCT, the values of A and r can be

selected through interpolation from Fig. 6 and then t_b can be calculated using Eq. (27). For example, at $C_0 = 2$ mg/L, $C_b = 0.5$ mg/L, EBCT = 6 min, and $Z = 20$ cm, the value of t_b from Eq. (27) was calculated to be 15.7 min, which was larger than that (=5.2 min) from Eq. (13).

Eq. (9) is the modified dose-response model presented by Yan et al. [14]. The nonlinear and linear regressions were performed in order to simulate the BTCs. The experimental BTCs along with the simulated BTCs of the nonlinear form of the modified dose-response model are presented in Fig. 5(b). The model parameters (a and q_0) determined from the simulations are presented in Table 6. The values of a and q_0 of the linear regression were different from the values of the nonlinear regression. The values of R^2, χ^2, and SSE indicated that the nonlinear regression was better at simulating the BTCs.

4. Conclusions

In this study, fixed-bed sorption models were clarified through comparative analysis using the breakthrough data from phosphate adsorption to slag filter media. In the literature, the original Bohart–Adams model was simplified to the convergent- and divergent-type models in order to be used for BTC analysis. However, the divergent-type model, which is equivalent to the Wolborska model, should not be used as the Bohart–Adams model, because it behaved totally different from the original model. Also, the Thomas and Yoon–Nelson models should not be used simultaneously with the Bohart–Adams model, because they are equivalent to the simplified convergent-type Bohart–Adams model and the parameters of both models can easily be calculated from the Bohart–Adams model parameters. The Bohart–Adams, Clark, and modified dose-response models could describe the breakthrough data relatively well with a high determination coefficient and a low chi-square coeffi-

cient. From this study, the Bohart–Adams, Clark, and modified dose-response models are recommended for the breakthrough data analysis, because these models can provide useful design parameters for the fixed-bed systems.

Acknowledgments

Nomenclature

a	— modified dose-response model constant	(–)
A	— Clark model constant	(–)
β	— mass-transfer coefficient of Wolbroska model	(1/min)
C_0	— concentration of adsorbate in the influent	(mg/L)
C_b	— breakthrough concentration	(mg/L)
C_e	— concentration of adsorbate in the solution at equilibrium	(mg/L)
C_t	— concentration of adsorbate in the effluent	(mg/L)
EBCT	— empty-bed contact time	(min)
k_{BA}	— Bohart–Adams rate constant	(L/min/mg)
k_T	— Thomas rate constant	(L/min/mg)
k_{YN}	— Yoon–Nelson rate constant	(/min)
K_F	— Freundlich constant	(L/g)
n	— Freundlich constant	(–)
N_0	— sorption capacity per unit volume of fixed-bed	(mg/L)
m	— number of experimental data points	(–)
ρ_b	— bulk density of adsorbent	(g/cm³)
q_0	— sorption capacity per unit mass of adsorbent	(mg/g)
q_e	— sorption capacity per unit mass of adsorbent at equilibrium	(mg/g)
Q	— flow rate	(L/min)
r	— Clark model constant	(1/min)
R^2	— determination coefficient	(–)
S	— cross-sectional area of fixed-bed	(cm²)
SSE	— sum of square error	(–)
t	— time	(min)
t_b	— breakthrough time	(min)
t_{total}	— total flow time	(min)
$t_{50\%}$	— time for 50% adsorbate breakthrough	(min)
τ	— time for 50% adsorbate breakthrough	(min)
U	— linear flow velocity	(cm/min)
χ^2	— chi-square coefficient	(–)
X	— mass of adsorbent	(g)
y_c	— predicted data obtained from the model	(–)
y_e	— experimental data	(–)
$\bar{y}_e$	— average of experimental data	(–)
Z	— bed depth	(cm)
Z_0	— critical-bed depth	(cm)

References

[1] J. Song, W. Zou, Y. Bian, F. Su, R. Han, Adsorption characteristics of methylene blue by peanut husk in batch and column modes, Desalination 265 (2011) 119–125.

[2] S. Singh, V.C. Srivastava, I.D. Mall, Fixed-bed study for adsorptive removal of furfural by activated carbon, Colloid. Surf. A 332 (2009) 50–56.

[3] R. Han, Y. Wang, X. Zhao, Y. Wang, F. Xie, J. Cheng, M. Tang, Adsorption of methylene blue by phoenix tree leaf powder in a fixed-bed column: Experiments and prediction of breakthrough curves, Desalination 245 (2009) 284–297.

[4] O. Hamdaoui, Dynamic sorption of methylene blue by cedar sawdust and crushed brick in fixed bed columns, J. Hazard. Mater. 138 (2006) 293–303.

[5] C.B. Lopes, E. Pereira, Z. Lin, P. Pato, M. Otero, C.M. Silva, J. Rocha, A.C. Duarte, Fixed-bed removal of Hg^{2+} from contaminated water by microporous titanosilicate ETS-4: Experimental and theoretical breakthrough curves, Microporous Mesoporous Mater. 145 (2011) 32–40.

[6] O. Hamdaoui, Removal of copper(II) from aqueous phase by Purolite C100-MB cation exchange resin in fixed bed columns: Modeling, J. Hazard. Mater. 161 (2009) 737–746.

[7] G.S. Bohart, E.Q. Adams, Some aspects of the behavior of charcoal with respect to chlorine, J. Am. Chem. Soc. 42 (1920) 523–544.

[8] Z. Aksu, F. Gönen, Biosorption of phenol by immobilized activated sludge in a continuous packed bed: Prediction of breakthrough curves, Process Biochem. 39 (2004) 599–613.

[9] H.C. Thomas, Heterogeneous ion exchange in a flowing system, J. Am. Chem. Soc. 66 (1944) 1664–1666.

[10] H.C. Thomas, Chromatography: A problem in kinetics, Ann. N.Y. Acad. Sci. 49 (1948) 161–182.

[11] Y.H. Yoon, J.H. Nelson, Application of gas adsorption kinetics I. A theoretical model for respirator cartridge service life, Am. Ind. Hyg. Assoc. J. 45 (1984) 509–516.

[12] R.M. Clark, Evaluating the cost and performance of field-scale granular activated carbon systems, Environ. Sci. Technol. 21 (1987) 573–580.

[13] A. Wolborska, Adsorption on activated carbon of p-nitrophenol from aqueous solution, Water Res. 23 (1989) 85–91.

[14] G. Yan, T. Viraraghavan, M. Chen, A new model for heavy metal removal in a biosorption column, Adsorp. Sci. Technol. 19 (2001) 25–43.

[15] M. Calero, F. Hernainz, G. Blazquez, G. Tenorio, M.A. Martin-Lara, Study of Cr(III) biosorption in a fixed-bed column, J. Hazard. Mater. 171 (2009) 886–893.

[16] R. Senthilkumar, K. Vijayaraghavan, M. Thilakavathi, P.V.R. Iyer, M. Velan, Seaweeds for the remediation of wastewaters contaminated with zinc(II) ions, J. Hazard. Mater. 136 (2006) 791–799.

[17] K. Pakshirajan, T. Swaminathan, Biosorption of copper and cadmium in packed bed columns with live immobilized fungal biomass of *Phanerochaete chrysosporium*, Appl. Biochem. Biotechnol. 157 (2009) 159–173.

[18] D. Karadag, E. Akkaya, A. Demir, A. Saral, M. Turan, M. Ozturk, Ammonium removal from municipal landfill leachate by clinoptilolite bed columns: Breakthrough modeling and error analysis, Ind. Eng. Chem. Res. 47 (2008) 9552–9557.

[19] V.C. Srivastava, B. Prasad, I.M. Mishra, I.D. Mall, M.M. Swamy, Prediction of breakthrough curves for sorptive removal of phenol by bagasse fly ash packed bed, Ind. Eng. Chem. Res. 47 (2008) 1603–1613.

[20] K.H. Chu, Fixed bed sorption: Setting the record straight on the Bohart–Adams and Thomas models, J. Hazard. Mater. 177 (2010) 1006–1012.

[21] Y.U. Han, C.G. Lee, J.A. Park, J.K. Kang, I. Lee, S.B. Kim, Immobilization of layered double hydroxide into polyvinyl alcohol/alginate hydrogel beads for phosphate removal, Environ. Eng. Res. 17 (2012) 129–134.

[22] C.G. Lee, J.A. Park, S.B. Kim, Phosphate removal from aqueous solutions using slag microspheres, Desalin. Water Treat. 44 (2012) 229–236.

[23] APHA (American Public Health Association), Standard Methods for the Examination of Water and Wastewater, APHA, Washington, DC, 1995.

[24] R.P. Han, D.D. Ding, Y.F. Xu, W.H. Zou, Y.F. Wang, Y.F. Li, L. Zou, Use of rice husk for the adsorption of congo red from aqueous solution in column mode, Bioresour. Technol. 99 (2008) 2938–2946.

[25] E. Guibal, R. Lorenzelli, T. Vincent, P.L. Cloirec, Application of silica gel to metal ion sorption: Static and dynamic removal of uranyl ions, Environ. Technol. 16 (1995) 101–114.

[26] W. Zhang, L. Dong, H. Yan, H. Li, Z. Jiang, X. Kan, H. Yang, A. Li, R. Cheng, Removal of methylene blue from aqueous solutions by straw based adsorbent in a fixed-bed column, Chem. Eng. J. 173 (2011) 429–436.

[27] R.A. Hutchins, New method simplifies design of activated-carbon systems, Chem. Eng. 20 (1973) 133–138.

[28] P.G. Priya, C.A. Basha, V. Ramamurthi, Removal of Ni(II) using cation exchange resins in packed bed column: Prediction of breakthrough curves, Clean—Soil, Air, Water 39 (2011) 88–94.